Extended Point Defects in Crystalline Materials: Ge and Si

N. E. B. Cowern,[1,*] S. Simdyankin,[1] C. Ahn,[1,†] N. S. Bennett,[1,‡] J. P. Goss,[1] J.-M. Hartmann,[2] A. Pakfar,[3,§] S. Hamm,[4] J. Valentin,[5] E. Napolitani,[6] D. De Salvador,[6] E. Bruno,[7] and S. Mirabella[7]

[1]*School of Electrical and Electronic Engineering, Newcastle University, Newcastle upon Tyne NE1 7RU, United Kingdom*
[2]*CEA, LETI, Minatec Campus, 38054 Grenoble, France*
[3]*ST Microelectronics, 850 rue Jean Monnet, 38920 Crolles, France*
[4]*Mattson Thermal Products GmbH, Daimlerstrasse 10, 89160 Dornstadt, Germany*
[5]*Probion Analysis, 37 rue de Fontenay, 92220 Bagneux, France*
[6]*CNR-IMM-MATIS and Dipartimento di Fisica, Università di Padova, Via Marzolo 8, 35131 Padova, Italy*
[7]*CNR-IMM-MATIS and Dipartimento di Fisica e Astronomia, Università di Catania, Via S. Sofia 64, 95123 Catania, Italy*

(Received 14 October 2012; published 8 April 2013)

B diffusion measurements are used to probe the basic nature of self-interstitial point defects in Ge. We find two distinct self-interstitial forms—a simple one with low entropy and a complex one with entropy $\sim 30\,k$ at the migration saddle point. The latter dominates diffusion at high temperature. We propose that its structure is similar to that of an amorphous pocket—we name it a *morph*. Computational modeling suggests that morphs exist in both self-interstitial and vacancylike forms, and are crucial for diffusion and defect dynamics in Ge, Si, and probably many other crystalline solids.

DOI: 10.1103/PhysRevLett.110.155501 PACS numbers: 61.72.J−, 61.72.Bb, 61.72.uf, 66.30.−h

A vast array of crystalline material properties arises from the behavior of atomic-scale point defects, yet these defects are poorly understood. Knowledge of simple point defects—single atoms added interstitially to, or missing from, an otherwise undisturbed lattice—is well established from quantum theoretical calculations and low-temperature experiments, but diffusion experiments hint that more complex entities may be involved at high temperatures relevant to industrial processing [1–5]. This Letter provides the first definitive evidence for these elusive complex defects and presents a specific physical model for their structure and diffusion.

Recent interest in Ge-based nanoelectronics has led to basic studies on diffusion [5–9] and implantation defects [10,11] in crystalline Ge. Most dopants in Ge are found to diffuse by vacancy mechanisms, with activation energies below that of vacancy-mediated self-diffusion (≈ 3.1 eV), but boron diffusion is an exception with an activation energy of ≈ 4.65 eV [6,12]. Experiments [5,7–9] show that boron diffuses via the reaction $\mathrm{B} + I \Leftrightarrow \mathrm{B}I$, where B represents substitutional boron, I the self-interstitial, and BI a mobile dopant-interstitial complex. The energetics involved is illustrated in Fig. 1.

The reduction in free energy on forming BI enables it to migrate a mean projected distance λ before dissociating to B and I. The mean number of jumps before dissociation depends on the energy difference between migration and dissociation of BI and the diffusional entropies of I and BI. In general,

$$\lambda = \lambda_0 \exp(-E_\lambda/kT), \tag{1}$$

where $E_\lambda = -(E_{\mathrm{self},X} + E_{\mathrm{barrier}} - E_{AX})/2$ and $\lambda_0 = (4\pi a/f_{AX})^{1/2} \exp[(S_{AX} - S_{\mathrm{self},X})/2k]$, A is the impurity (here, boron), X the point defect driving AX diffusion (here, I), a the capture radius for the forward reaction, f_{AX} the diffusion correlation factor (~ 1), E_{AX}, S_{AX}, $E_{\mathrm{self},X}$, $S_{\mathrm{self},X}$ the activation energies and entropies of impurity diffusion and self-diffusion via the species AX and X, respectively, and E_{barrier} the energy barrier to the forward reaction (Fig. 2). Similarly to the case of Si, where $E_\lambda = -0.5$ eV [13] and $E_{\mathrm{barrier}} < 0.05$ eV [14], recent experiments in Ge in the temperature range $T > 0.65T_m$ yield E_λ in the range -0.8 [7] to -0.6 eV [8] with $E_{\mathrm{barrier}} \approx 0$ eV [7–9]. Using Eq. (1) above this implies $E_{\mathrm{self},I} - E_{\mathrm{B}I} \approx 1.2$ to 1.6 eV, and since $E_{\mathrm{B}I} \approx 4.65$ eV [6], we find $E_{\mathrm{self},I} \approx 5.85$ to 6.25 eV. This is nearly 2 eV higher than predicted from first principles [15], and more than 1 eV higher than $E_{\mathrm{self},I}$ in Si [16].

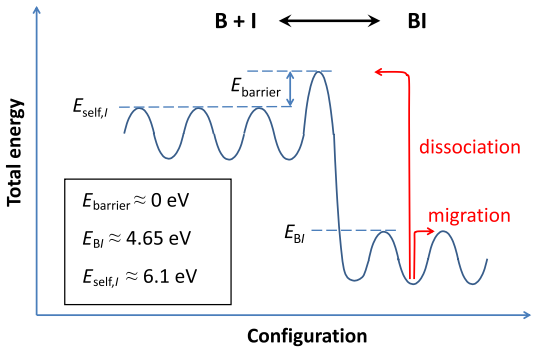

FIG. 1 (color online). Schematic of total energy versus configuration for the reaction mediating B diffusion in Ge. Also shown are energies inferred from previous experiments. $E_{\mathrm{B}I}$ and $E_{\mathrm{self},I}$ are the respective energies of BI and I at their migration saddle points, relative to that of substitutional B.

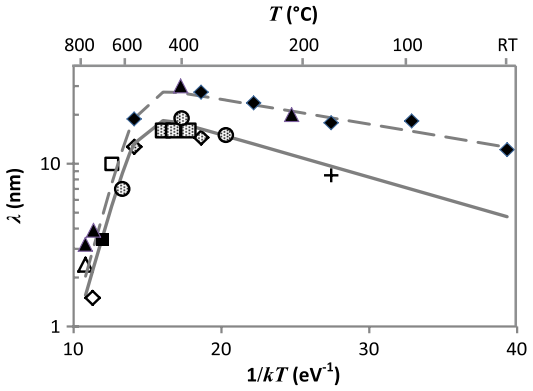

FIG. 2 (color online). Migration length of BI in Ge versus $1/kT$. Open symbols: thermal diffusion data from Ref. [7] (diamond) and Ref. [9] (triangle), and oxide precipitate-enhanced diffusion data from Ref. [17] (square). Shaded symbols: postimplant diffusion data from this work (circles), Ref. [7] (diamonds), and Ref. [8] (squares). Solid symbols: H-irradiation enhanced diffusion (RED) data from Ref. [7] (diamonds), Ref. [9] (triangles), and Ref. [17] (square). Cross symbol: O-RED data from Ref. [18] (O gives less ionization than H per atomic displacement). The curves are fits of Eq. (1) generalized to account for competing dissociation channels to two self-interstitial forms, I and $\mathcal{I}$. The best fit under nonirradiation conditions (solid curve) is obtained with $E_\lambda = (-0.725 \pm 0.10)$ eV, $\lambda_0 = 0.62$ pm for $\mathcal{I}$, and $E_\lambda = (0.06 \pm 0.02)$ eV, $\lambda_0 = 50$ nm for I. Under RED conditions (dashed curve) the fitted values of E_λ shift 0.025 eV in the negative direction. This could be accounted for by a reduction of 0.05 eV in the migration energy of BI under H irradiation.

At lower temperatures, data on B diffusion in Ge show a quite different behavior of the migration length [7–9]; as Fig. 2 shows, E_λ changes from about -0.75 eV at $T > 550$ °C to about $+0.06$ eV at lower T. It has previously been suggested that the high-T results reflect the true activation energy while the low-T results are an artifact of BI trapping at C or O atoms in the MBE-grown Ge used in Ref. [7]. Here we propose an alternative view; the low-T results arise from dissociation into a different self-interstitial species with lower activation energy and entropy.

To test this idea we have repeated the experiments, now using CVD-grown epitaxial Ge in which trap concentrations are definitively too low to affect B diffusion [12]. Extracted values of λ are shown in Fig. 2, together with previous results [7–9,17,18]. Our data points are perfectly consistent with the earlier results, despite the absence of traps—thus strongly supporting our proposal of two self-interstitial species. Assuming $E_{BI} = 4.65$ eV over the full temperature range of Fig. 2, we have fitted the results in Fig. 2 with a formula based on two self-interstitial forms [12]. For the low-T self-interstitial, which we label I, we find $E_{\text{self},I} \approx 4.55$ eV and $S \approx 4\ k$, whereas for the high-T self-interstitial, labeled $\mathcal{I}$, $E_{\text{self},I} \approx 6.1$ eV and $S \approx 30\ k$. The low-T value of $E_{\text{self},I}$ agrees with first-principles calculations for a localized self-interstitial in Ge [4] and the corresponding entropy value confirms I is indeed a simple point defect. In contrast, the high-T value is unexplained by theory and its entropy has an extreme, record-breaking value. One way to explain this would be to invoke premelting effects, i.e., melting fluctuations that occur close to the transition to the liquid phase. However, this explanation seems to be ruled out by the near-constant activation energy over the observed temperature range, and the fact that this range is far below the melting point. We propose instead that $\mathcal{I}$ has a complex, thermodynamically stable structure incorporating a number of atoms from the lattice.

The sharpness of the transition between the two diffusion regimes can be explained if there is a reaction barrier between the two defect forms. Figure 3 shows a model for the energy and entropy of self-interstitials that extend over different volumes of the lattice (N atoms occupying a volume normally occupied by $N-1$ lattice atoms). At low temperature the simple form is dominant, while at high temperature the complex form dominates.

It is obviously of great interest to know what physical form the complex defect takes, and a simple model of a small disordered region leads to interesting semiquantitative predictions. A rough upper limit on the number of atoms in the defect is $N < S_{\text{self},I}/s_f$, where s_f is its formation entropy per atom and the inequality applies because $S_{\text{self},I}$ includes both formation and migration entropy. Applying this to Seeger's liquid drop model of an extended

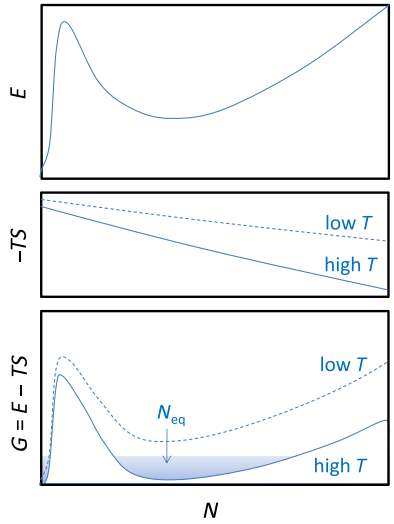

FIG. 3 (color online). Schematic diagram of enthalpy, E, entropic energy term, $-TS$, and resultant Gibbs free energy, G, for the self-interstitial as function of size, illustrating how a simple structure may dominate at low T and a complex structure dominate at high T. N represents the number of lattice atoms incorporated into the defect; zero or one in the case of a compact self-interstitial (e.g., a simple or split interstitial), but much larger in the case of an amorphous pocket, though this still only contains one excess atom.

point defect [1], s_f would be the entropy of fusion, 3.6 k/atom, resulting in a value of $N < 8$. This is too small to behave like a bulk liquid as confined liquids become solidlike [19], with much lower entropy and internal energy per atom.

Thus it is interesting to consider a larger structure, with a formation energy per atom rather close to that of the crystalline solid, yet with high entropy. We postulate an extended region, or *morph*, having regular coordination with the surrounding lattice but containing the basic building blocks found in amorphous material (for example, in Ge and Si, four, five, six and/or seven-membered rings). In the case of an interstitial-like defect (i morph) the structure would contain one extra atom and in a vacancylike defect (v morph) there would be a deficit of one atom.

A very rough estimate of the formation energy of morphs, independent of specific structures, can be obtained using a semiempirical, macroscopic approach. We assume a spherical inclusion and write

$$E_f = H_c N + E_\varepsilon(\mu) + E_{\mathrm{bd}};$$
$$\mu = (1+\alpha)(N+n)/N - 1$$

where H_c is the heat of crystallization of the amorphous phase, E_ε is the misfit strain energy, and E_{bd} is an additional bond distortion energy [12]. Literature values for H_c are significantly scattered [20,21] and not always mutually consistent with published entropy values—here we use $H_c \approx 0.1$ eV/atom for Ge and 0.12 eV/atom for Si. The misfit μ contains two factors, one related to the volume mismatch α between crystalline and amorphous phases ($\alpha \approx 1.5\%$ for Si and Ge), the other to the excess number of atoms in the defect ($n = 1$ for $\mathcal{I}$, $n = -1$ for $\mathcal{V}$, the v morph). Strain energy is roughly estimated from the Birch-Murnaghan high-pressure equation of state [22], assuming the defect is surrounded by a rigid matrix [12]. Finally, we choose $E_{\mathrm{bd}} = 1$ eV to match our measured activation energy for $\mathcal{I}$ in Ge. This procedure yields rough estimates of E_f for $\mathcal{I}$ and $\mathcal{V}$ in Ge and Si as shown in Figs. 4(a) and 4(e). Energy is minimized when strain energy (which decreases with N at small N values) equals constitutive energy (which increases monotonically with N).

Because entropy increases with N, at finite T the minimum in Gibbs free energy occurs at larger N. For $\mathcal{I}$, an entropy of 1 k/atom in Si or Ge (assumed equally distributed between formation and migration entropy) and a value of $N \approx 30$ in Ge gives good agreement with our experiment-based diffusion entropy estimate of 26.6 k. For the sake of precision it is worth noting that, during morph migration, the center of mass of the defect moves by only a fraction of the normal self-interstitial jump length per rebonding event [12]. This leads to a small correction of about 2.5 k in the entropy inferred from our experiment; i.e., we obtain $S \approx 30$ k. However, as our model is inherently approximate and our estimated diffusion entropy per atom is drawn from scattered literature data [23] our results

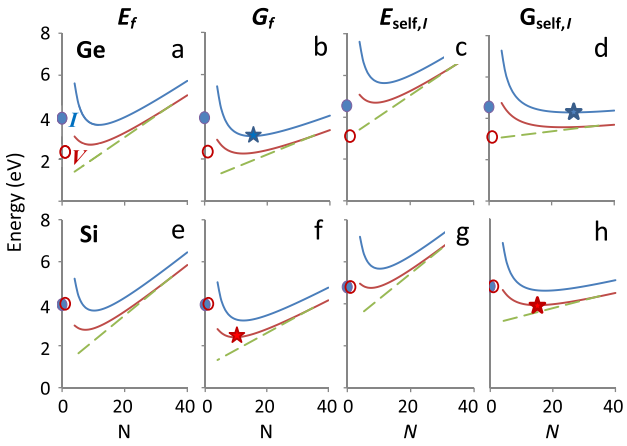

FIG. 4 (color online). Energy and Gibbs free energy (at 700 °C) of defect formation [left-hand panels: (a),(b),(e),(f)] and self-diffusion [right-hand panels: (c),(d),(g),(h)] for Ge (top) and Si (bottom), as functions of N. Values for simple point defects are shown at left of each panel (I—closed symbol; V—open symbol). Estimated values for morphs are shown by solid curves ($\mathcal{I}$—upper curve, $\mathcal{V}$—lower curve). Stars indicate the free-energy minima for morphs in their stable state (b),(f), and at the diffusion saddle point (d),(h). Dashed lines show values when strain energy is omitted.

should not be seen as exact predictions but rather as an indication of trends.

We now take a closer look at the trends shown in Fig. 4, and draw comparisons with published experimental data where available. As shown in the left half of Fig. 4, the predicted formation energies of morphs are comparable to those of simple point defects and their Gibbs free energies are lower. This suggests the predominant vacancy and self-interstitial species in Si might also be morphs. Low G_f values for morphs could account for numerous unexplained experimental observations. For example, the huge scatter of literature data for point-defect concentrations and diffusivities in Si could arise from different coupling between populations of low-concentration, fast-diffusing simple point defects and high concentration, slow-diffusing morphs in different experiments. This interplay could be crucial for understanding defect formation during crystal growth and electronic device fabrication, and explain discrepancies between point-defect parameters needed to model processes at different length, time, and temperature scales.

The relative contributions of simple point defects and morphs to diffusion also depend on their respective migration energies. Morph migration relies on peripheral rebonding, the process involved in solid-phase epitaxy (SPE). Hence, for a rough estimate of morph migration energies we use the SPE activation energies for Ge [24] and Si [25]: 2.1 eV and 2.85 eV, respectively. As shown in the right half of Fig. 4, for $\mathcal{I}$ this leads to E_{self} values of around 6 eV in Si and Ge, but a significantly lower G_{self} owing to the large entropies involved.

In the case of $\mathcal{V}$ we find a self-diffusion activation energy of about 5 eV in Si and Ge. This indicates the compact vacancy, with activation energy 3.1 eV, dominates self-diffusion in Ge, a result consistent with experimental data showing a single activation energy over several hundred degrees [26]. However, in Si, our model suggests $\mathcal{V}$ may contribute significantly. Our estimated 5 eV activation energy is close to the experimental value of 4.86 eV for vacancy-mediated self-diffusion in Si at high T [4]. Moreover, our high migration-energy value of 2.85 eV for the morph in Si agrees quite well with the vacancy migration energy observed experimentally at high T [3] (≈ 1.65 eV, contrasting with ≈ 0.5 eV at low T). This consistent picture of a morph-type vacancy at high T and a simple vacancy at low T resolves previous controversy on vacancy-mediated self-diffusion [27]. This point is discussed in further detail in Ref. [12].

It is also instructive to compare our modeled entropy values with published experimental data. Our values of $\approx 9\ k$ for $\mathcal{V}$ in Si, 16 k for $\mathcal{I}$ in Si, and 30 k for $\mathcal{I}$ in Ge are well matched by experimental high-T diffusion entropy values of 10 k for $\mathcal{V}$ in Si [4], 12 k for $\mathcal{I}$ in Si [4], and about 30 k for $\mathcal{I}$ in Ge (our experiments), respectively [star symbols in Figs. 4(f) and 4(d), again attributing 1 k/atom].

Finally, our model may resolve several further unexplained features of diffusion and defect dynamics in Si and Ge which at first sight would seem unrelated. First, it predicts broadly similar free energies of formation, migration, and thus self-diffusion for $\mathcal{I}$ and $\mathcal{V}$ in the same material, because the free energy of a morph is related to the number of atoms involved. For example, a morph with 29 atoms on a 30-atom crystalline footprint is a $\mathcal{V}$, while one with 31 atoms is an $\mathcal{I}$; these will have similar configurational free energies of formation and migration. This neatly explains, for the first time, the notable coincidence of interstitial and vacancy-mediated self-diffusion coefficients in Si at high T [4]. Second, the predominance of a complex, high-entropy self-interstitial in Ge may explain the anomalously low recombination rate for self-interstitials at the Ge surface [5]. If $\mathcal{I}$ recombines at specific localized sites, as is thought to occur with simple point defects, recombination will be inhibited by a free-energy barrier as the defect shrinks and annihilates. Third, the low formation energies of interstitial and vacancy-type morphs in Ge may explain the ease with which Ge amorphizes during ion bombardment with energy density above about 0.1 eV/atom [28]. In this picture, rather than forming predominantly simple point defects that can migrate and recombine, the bombardment produces $\mathcal{I}$ and $\mathcal{V}$ morphs that are immobile at room temperature and so accumulate and ultimately overlap.

It is clearly important to test the predictions of our semiempirical model against atomistic calculations. We have therefore conducted initial molecular dynamics (MD) calculations, using a potential that gives an energy gap between the crystalline and relaxed amorphous phases of about 0.1 eV [29], close to experimentally observed values for Si and Ge. This choice is crucial to success as substantially higher energy gaps (≈ 3 times higher with the frequently used Stillinger-Weber potential [30]) incorrectly penalize morph formation. We find characteristic morph structures that are thermally stable and mobile at high temperature, and migrate by shape shifting through numerous configurations of similar energy. By way of illustration, two snapshots of the same self-interstitial defect, taken 20 ps apart during diffusion at $T \approx 0.95\ T_m$, are shown in Fig. 5. At lower temperatures similar morph structures are seen and occasional transitions between the compact and morph forms occur. Broadly similar results are found for vacancies, with a slightly smaller defect size and fewer structural permutations—again consistent with our predicted trend. A full discussion of MD calculations for native defects in the diamond lattice at high temperature will be presented elsewhere.

In conclusion, at high temperature the self-interstitial in Ge is a complex, mutable yet robust structure of dimensions $\sim$1 nm, with a structure similar to an amorphous pocket. Analogous morph structures are expected to exist for both the self-interstitial and vacancy in Si. More generally, there is the exciting possibility that morphs occur throughout the wide range of crystalline materials that have a small amorphous-crystalline energy gap, including important geophysical materials like ice and advanced technological materials such as high-κ dielectrics. Since point-defect properties are fundamental to materials behavior in applications from industrial processing to glacier dynamics we believe this novel class of point defects merits extensive further study.

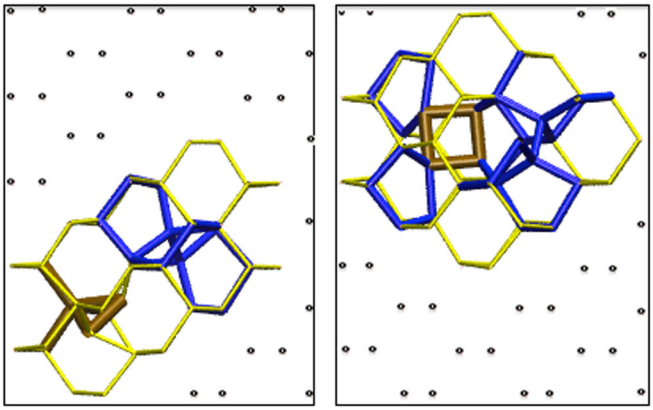

FIG. 5 (color online). Two MD simulation frames, separated by 20 ps, showing migration of an i morph through part of a 10,000 atom simulation volume. Seven-membered rings are shown with thin (yellow) "bonds", five-membered with thicker (blue) bonds, and fewer-membered with the thickest bonds. Dots mark atomic positions on the surrounding diamond lattice.

We are grateful to Paul Coleman and Charlene Edwardson for carrying out positron annihilation measurements, to David Drabold and Yuting Li for sending us some of their amorphous Si models, to Normand Mousseau and Ali Kerrache for sharing their FORTRAN code, which we modified for the ring analysis used in Fig. 5, and to Robert Falster, Vladimir Voronkov, and Alain Claverie for illuminating discussions. The research leading to these results received funding from the European Union Seventh Framework Programme (FP7/2007-2013) under Grant No. 258547 (ATEMOX).

*nick.cowern@ncl.ac.uk

†Present address: Samsung Semiconductor Inc., 75 W Plumeria Dr., San Jose, CA 95134, USA.

‡Present address: Nanomaterials Processing Laboratory, School of Electronic Engineering, Dublin City University, Glasnevin, Dublin 9, Ireland.
Address from July 2013: Institute of Mechanical, Process and Energy Engineering, Heriot-Watt University, Edinburgh EH14 4AS, United Kingdom.

§Present address: GLOBALFOUNDRIES, Wilschdorfer Landstrasse 101, 01109 Dresden, Germany.

[1] A. Seeger, Phys. Status Solidi B **248**, 2772 (2011).
[2] A. Seeger, Radiat. Eff. **9**, 15 (1971).
[3] H. Bracht, J. F. Pedersen, N. Zangenberg, A. N. Larsen, E. E. Haller, G. Lulli, and M. Posselt, Phys. Rev. Lett. **91**, 245502 (2003).
[4] A. Ural, P. B. Griffin, and J. D. Plummer, Phys. Rev. Lett. **83**, 3454 (1999).
[5] H. Bracht, S. Schneider, J. N. Klug, C. Y. Liao, J. L. Hansen, E. E. Haller, A. N. Larsen, D. Bougeard, M. Posselt, and C. Wündisch, Phys. Rev. Lett. **103**, 255501 (2009).
[6] S. Uppal, A. F. W. Willoughby, J. M. Bonar, N. E. B. Cowern, T. Grasby, R. J. H. Morris, and M. G. Dowsett, J. Appl. Phys. **96**, 1376 (2004).
[7] E. Bruno, S. Mirabella, G. Scapellato, G. Impellizzeri, A. Terrasi, F. Priolo, E. Napolitani, D. De Salvador, M. Mastromatteo, and A. Carnera, Phys. Rev. B **80**, 033204 (2009).
[8] E. Napolitani *et al.*, Appl. Phys. Lett. **96**, 201906 (2010).
[9] G. G. Scapellato, E. Bruno, A. J. Smith, E. Napolitani, D. De Salvador, S. Mirabella, M. Mastromatteo, A. Carnera, R. Gwilliam, and F. Priolo, Nucl. Instrum. Methods Phys. Res., Sect. B **282**, 8 (2012).
[10] G. Bisognin, S. Vangelista, and E. Bruno, Mater. Sci. Eng. B **154–155**, 64 (2008).
[11] A. Claverie, S. Koffel, N. Cherkashin, G. Benassayag, and P. Scheiblin, Thin Solid Films **518**, 2307 (2010).
[12] See Supplemental Material at http://link.aps.org/supplemental/10.1103/PhysRevLett.110.155501 for further details on our experiments, analysis, and physical considerations.
[13] N. E. B. Cowern, K. T. F. Janssen, G. F. A. van de Walle, and D. J. Gravesteijn, Phys. Rev. Lett. **65**, 2434 (1990).
[14] N. E. B. Cowern, G. Mannino, P. A. Stolk, F. Roozeboom, H. G. A. Huizing, J. G. M. van Berkum, F. Cristiano, A. Claverie, and M. Jaraíz, Mater. Sci. Semicond. Process. **2**, 369 (1999).
[15] C. Janke, R. Jones, S. Öberg, and P. R. Briddon, J. Mater. Sci. Mater. Electron. **18**, 775 (2007).
[16] H. Bracht, E. E. Haller, R. Clark-Phelps, Phys. Rev. Lett. **81**, 393 (1998).
[17] G. G. Scapellato, Ph.D. thesis, University of Catania, 2011.
[18] E. Bruno, S. Mirabella, G. Scapellato, G. Impellizzeri, A. Terrasi, F. Priolo, E. Napolitani, D. De Salvador, M. Mastromatteo, and A. Carnera, Thin Solid Films **518**, 2386 (2010).
[19] J. Gao, W. D. Luedtke, and U. Landman, Phys. Rev. Lett. **79**, 705 (1997).
[20] A. Gabriel, Ph.D. thesis, Technical University of Dresden, 2008.
[21] F. Kail, J. Farjas, P. Roura, C. Secouard, O. Nos, J. Bertomeu, and P. Roca i Cabarrocas, Phys. Status Solidi **5**, 361 (2011).
[22] F. Birch, Phys. Rev. **71**, 809 (1947).
[23] R. L. C. Vink and G. T. Barkema, Phys. Rev. Lett. **89**, 076405 (2002).
[24] D. Y. C. Lie, J. Electron. Mater. **27**, 377 (1998).
[25] M. Bauer, M. Oehme, M. Sauter, G. Eifler, and E. Kasper, Thin Solid Films **364**, 228 (2000).
[26] G. Vogel, G. Hettich, and H. Mehrer, J. Phys. C **16**, 6197 (1983).
[27] G. D. Watkins, J. Appl. Phys. **103**, 106106 (2008).
[28] C. Claeys and E. Simoen, in *Extended Defects in Germanium: Fundamental and Technological Aspects*, Springer Series in Materials Science Vol. 118 (Springer, New York, 2009), Ch. 5, 241–292.
[29] J. Tersoff, Phys. Rev. B **37**, 6991 (1988).
[30] M. J. Caturla, T. Diaz de la Rubia, and G. H. Gilmer, Nucl. Instrum. Methods Phys. Res., Sect. B **106**, 1 (1995).